Comparison of Polystyrene, Poly(styrene/Acrylonitrile), High-Impact Polystyrene, and Poly(acrylonitrile/Butadiene/Styrene) with Respect to Tensile and Impact Properties

MITSURU YOKOUCHI, SHINICHI SETO, and YASUJI KOBAYASHI,
Department of Industrial Chemistry, Faculty of Technology, Tokyo Metropolitan University, Fukazawa, Setagaya-ku, Tokyo 158, Japan

Synopsis

The tensile behaviors of polystyrene (PS), poly(styrene/acrylonitrile) (SAN), high-impact polystyrene (HIPS), and poly(acrylonitrile/butadiene/styrene) (ABS) were examined systematically in the wide range of strain rate, 1.7×10^{-4}–13.1 m/s. When glassy and brittle PS was a criterion, the incorporation of a polar group (SAN) only strengthened the hardness, and the fracture mode was the same as for PS. The introduction of dispersed rubber particles (HIPS) weakened the hardness a little but offered a new deformation mechanism, i.e., microcrazing (whitening), and contributed to the improvement of impact strength. In the heterogeneous system, the enhancement of matrix strength [e.g., preorientation or blending with poly(phenylene oxide) for HIPS] makes possible another deformation mechanism, i.e., shear band formation (cold drawing), which is superior to microcrazing for achieving higher impact strength. ABS, which incorporates concurrently two factors (polar group to matrix phase and dispersed rubber particles), can be regarded as an enhancement of the matrix strength of HIPS. In spite of the remarkable magnitude of its impact strength compared with that of the other three polymers, the deformation mechanism of ABS was limited to microcrazing. This indicated that only the introduction of a polar group (as nitrile group) could not strengthen the matrix as much as preorientation or blending with poly(phenylene oxide).

INTRODUCTION

The homopolymer of styrene (PS) exhibits brittle fracture and low impact toughness at room temperature. To make up for this deficiency, two measures are taken. First, the breaking stress is reinforced by the introduction of polar groups. For example, styrene and acrylonitrile are copolymerized (SAN). Secondly, the strain up to fracture is increased without an accompanying lowering of strength. This can be performed by the addition of rubber in particle form to polystyrene. It is important that the dispersed rubber particles are grafted onto polystyrene chains (not a simple milling-in of rubber with PS matrix). Poly(acrylonitrile/butadiene/styrene) (ABS) is a two-phase material consisting of elastomer particles in a glassy polymer matrix of SAN. ABS can be interpreted as a polymer in which the two measures described above are combined. Correlations among the chemical components of PS, SAN, HIPS, and ABS are schematized (Fig. 1).

The aim of the present study is to investigate how the mechanical properties of a polymer change (1) by the introduction of a polar group, (2) with the incor-

Journal of Applied Polymer Science, Vol. 28, 2209–2216 (1983)
 CCC 0021-8995/83/072209-08$01.80

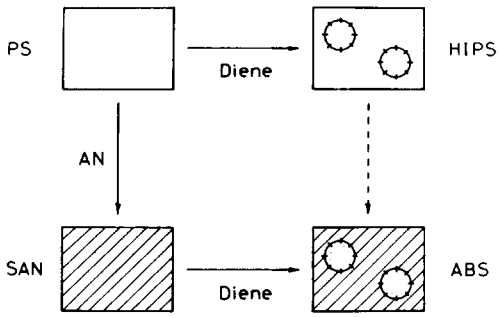

Fig. 1. The relationship of chemical components among PS, SAN, HIPS, and ABS.

poration of dispersed rubber particles which are grafted onto the matrix polymer chains, and (3) by the concurrent introduction of the factors (1) and (2), when polystyrene is primarily a criterion of the mechanical properties. The mechanical testing was limited to measurements of tensile and impact tensile properties at room temperature, where the shape of specimen and the deformation mode were all the same in the wide range of deformation speeds (1.7×10^{-4}–13.1 m/s).

EXPERIMENTAL

Specimens

The resins used were as follows; granules of (1) atactic PS (Styron 666, Asahi Dow), (2) SAN (SAN-C, Mitsubishi Montsant Chem.), (3) HIPS (Styron 470, Asahi Dow), and (4) ABS (JSR-82, Japan Synthetic Rubber). The chemical elemental analyses roughly indicated the monomer ratios (Table I). These granules were compression-molded into sheets about 250 μm thick, followed by quenching in ice water. A heated cutter was used to prepare specimens to avoid unnecessary cracks at the cut plane. Since both ends were reinforced by aluminum adhesive tape, the practical specimen dimensions were 5×58 mm. The specimens were used for both low and high (impact) speed tensile tests.

Tensile Breaking Tests

For impact tensile tests, a flywheel-type tensile impact tester was used, of which details of the characteristics and operating procedures have been reported previously.[1] The tensile speeds were controlled by changing the revolutions of

TABLE I
Monomer Ratios of PS, SAN, HIPS, and ABS, Calculated from Chemical Elemental Analyses (mol %)

Material	ST	AN	BD
PS	100	—	—
SAN	60	40	—
HIPS	79	—	21
ABS	44	32	24

the flywheel and in the present study were in the range of 1.3–13.1 m/s. For low speeds, a conventional tensile tester was utilized, which covered the rate of deformation from 1.7×10^{-4} to 2.8×10^{-2} m/s. This enabled us to test over five decades of strain rate ($0.29–2.3 \times 10^4$ %/s). The experiments were conducted at almost constant temperature ($23 \pm 1°C$) and around 50% RH. The number of specimens tested per each strain rate was 10 for the high speeds and 5 for the low speeds, and the arithmetic mean and estimated standard deviation were calculated from the set of observations. The obtained stress–strain curve gave the following four mechanical quantities: (1) modulus of elasticity, E; (2) maximum load at yield or breaking, σ_m; (3) extension to failure, ϵ_b; and (4) breaking energy indicated by the area under the curve, S_b.

RESULTS AND DISCUSSION

Young's Modulus

Figure 2 shows the strain rate dependencies of the initial elasticities (E) calculated from the slopes of stress–strain curves. The elasticity of SAN is higher than that of PS in the whole range of deformation speeds. The introduction of a polar group raises the Young's modulus or hardness. Inversely, the elasticity of HIPS, which contains the dispersed rubber particles, is lower than that of PS. This may be simply interpreted by the apparent reduction of hard PS matrix content. The concurrent introduction of polar groups to the matrix element and dispersed rubber particles, which just correspond to ABS, lead to the mu-

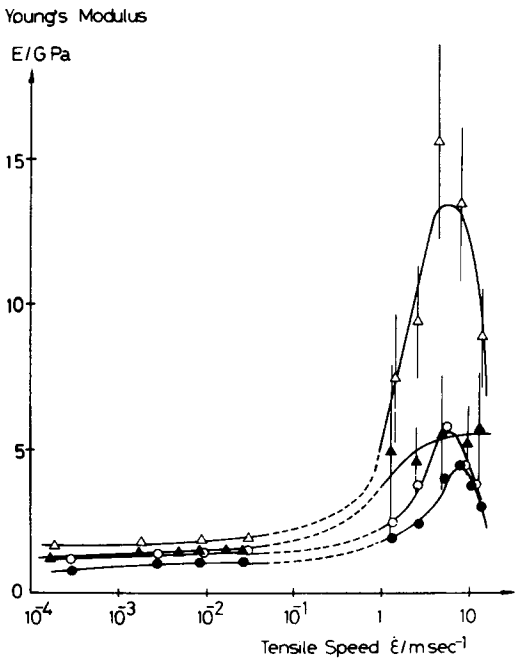

Fig. 2. Strain rate dependencies of tensile Young's modulus: (○) PS; (△) SAN; (●) HIPS; (▲) ABS.

tually compensative effect upon the hardness of the resin. The Young's modulus of the present ABS is a little higher than that of PS. The values may be dependent on the acrylonitrile content and the quantity of rubber particles.

In the present stage, it could not be judged whether the abrupt decrease in Young's modulus of some polymers in the higher impact region is due to the essential properties of the polymers, the preparation method of the test specimens, or the performance of the testing apparatus.

Maximum Load

Figure 3 shows the strain rate dependencies of the maximum loads (σ_m), which correspond to the yield stress or the breaking stress for the case of brittle fracture. Compared with PS and SAN, the maximum load is enhanced by the incorporation of a polar group. On the other hand, the maximum load of HIPS deteriorated by the introduction of the rubber phase, compared with PS. For the case of ABS, the situation differed slightly. The maximum load of ABS in the impact deformation region was superior to that of SAN, which is the matrix element of ABS. This can be interpreted as follows. The maximum load is determined by the initial slope of the stress–strain curve and the deformation quantity up to the point indicating the maximum load. In ABS, the initial slope is a little larger than that of PS, and the deformation up to the yield point is larger than that of SAN. The latter was due to the whitening mechanism, which is for the first time possible in the presence of the dispersed rubber particles grafted on to the matrix polymer chains. This whitening mechanism will be discussed in

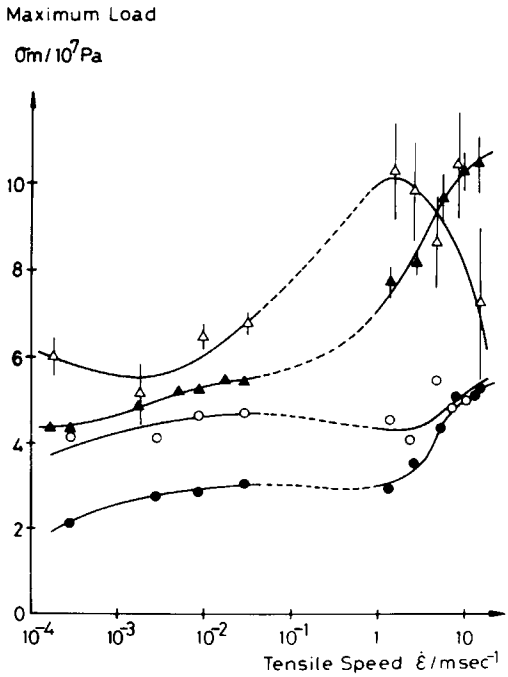

Fig. 3. Strain rate dependencies of maximum tensile stress: (○) PS; (△) SAN; (●) HIPS; (▲) ABS.

the following section. These two factors may contribute to the strengthening of the maximum load in the impact speed region. Judging from the similar patterns of the strain rate dependencies of the maximum loads of HIPS and ABS, the low value of HIPS was due to the relatively weaker matrix component, PS, as compared to SAN.

Breaking Strain

Figure 4 shows the strain rate dependencies of the breaking strains (ϵ_b). The patterns of PS and SAN were similar and indicated simply a brittle fracture, which was almost independent of the deformation speeds. On the contrary, HIPS and ABS, which contain the dispersed rubber particles, indicated the characteristic patterns. Since the breaking strain is plotted on the same scale at the low and high (impact) speeds (Fig. 4), there seems to be almost no difference among PS, SAN, HIPS, and ABS. However, the observed subtle difference of ϵ_b at the impact speeds is very important for the enhancement of impact strength.

Breaking Energy

Figure 5 shows the strain rate dependencies of the breaking energies (S_b). This is determined approximately as a product of the maximum load and the breaking strain. Since the values of σ_m varied in the region of the impact speeds, the characteristic patterns of ϵ_b were magnified for the case of S_b. The patterns of PS and SAN were similar. The difference in the magnitude resulted from the maximum loads in Figure 3. HIPS showed the V-type pattern with the sharp minimum around the deformation speed of 10 m/s. ABS gave the U-type pattern

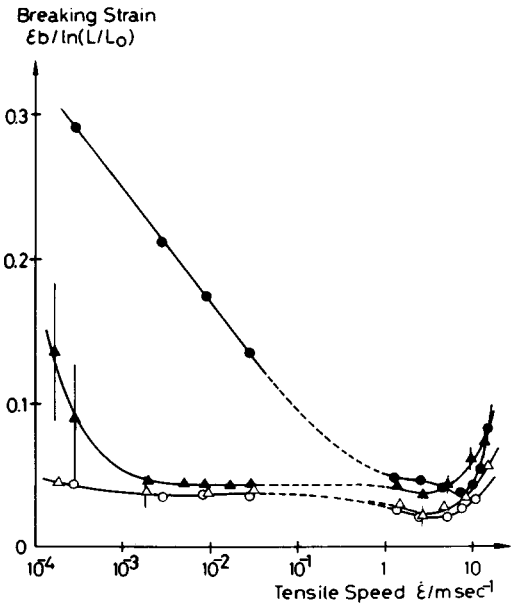

Fig. 4. Strain rate dependencies of breaking strain: (○) PS; (△) SAN; (●) HIPS; (▲) ABS.

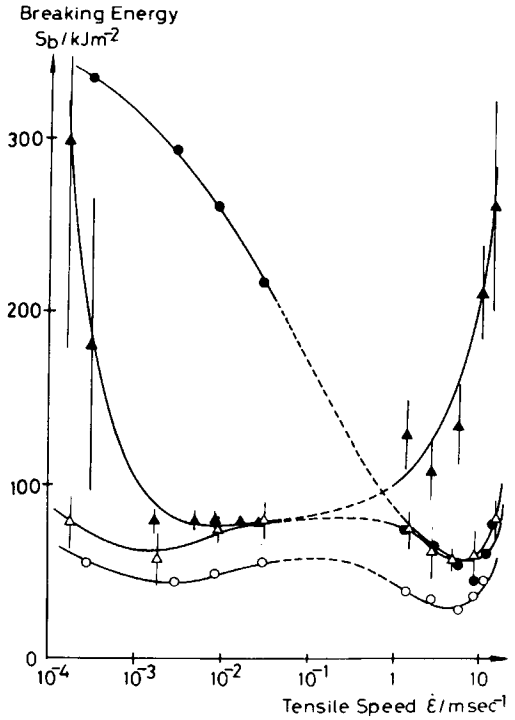

Fig. 5. Strain rate dependencies of breaking energy: (○) PS; (△) SAN; (●) HIPS; (▲) ABS.

with the loose bottom extending over the wide range of deformation speeds from about 10^{-3} to 2 m/s. The remarkable magnitude of ABS in the impact speeds implies that ABS is fit for the uses necessitating impact strength. The difference in the components of HIPS and ABS is in the superfluous presence of acrylonitrile composition in the latter matrix. The strengthening of the matrix may not be responsible for the distinct strain rate dependencies of HIPS (V type) and ABS (U type). It would appear that a synergistic effect emerges upon the concurrent incorporations of a polar group and dispersed rubber particles.

Fracture Mechanism

The results of the tensile breaking tests described above are discussed in connection with the deformation mechanism up to fracture. Figure 6 summarizes the mechanisms clarified so far.[2-4] PS creates microcrazes which grow instantaneously from the initial deformation state, to great microcracks, resulting in a brittle fracture. For HIPS, the equatorial zones of the dispersed rubber particles function as stress concentration points. From the boundary region of rubber phase and glassy matrix, a tremendous number of microcrazes occur, and they are observed as a whitening phenomenon.

It is of interest to determine the deformation mechanism which arises when the critical stress for the generation of microcrazes (σ_{mc}) is elevated by changing the matrix strength. There is a difference of Poisson's ratio between components

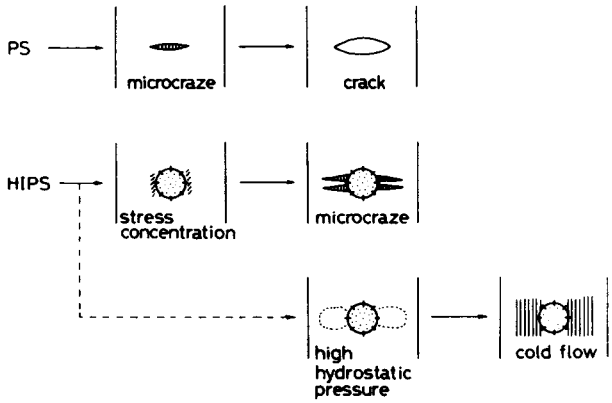

Fig. 6. Tensile deformation mechanisms of PS and HIPS.

in HIPS. During tensile deformation, the rubber phase does not change its volume while the glassy matrix dilates. This leads to a state of very high hydrostatic pressure at the boundary of rubber and glassy matrix phases. The stronger the critical stress up to the occurrence of microcraze at the glassy matrix, the higher the hydrostatic pressure. Generally, the stress of microcrazing (σ_{mc}) and that of shear band formation (σ_{sb}) compete with each other in the glassy polymer.[5,6] At atmospheric pressure, σ_{mc} is smaller than σ_{sb} and the fracture mode is brittle-like. When environmental pressure is very high, the order reverses and a ductile-like fracture takes precedence over a brittle-like one. Usually, the strain quantity until fracture is far larger in the shear band formation than in microcrazing. Hence, the shear band formation, i.e., cold drawing, is advantageous for the improvement of impact strength. Therefore, the key point is an enhancement of σ_{mc} as much as possible and the avoidance of excess stress concentration at the boundary of rubber and glassy matrix phases.

For HIPS, there is a procedure for realizing the enhancement of σ_{mc}; that is, preorientation at the temperature near the T_g.[7] By predrawing, the polymer chains of the matrix phase orient along the stretching direction. This suppresses the occurrence of microcrazes along the direction perpendicular to the stress field. Furthermore, hot drawing deforms the rubber particle from sphere to prolate spheroid and brings an increase in apparent radius of curvature at the equatorial zone of the dispersed rubber particle. This settled deformation decreases the degree of stress concentration and indirectly enhances the critical stress for microcrazing. These changes lead to higher hydrostatic pressure, and the cold drawing phenomenon (shear band formation) can be, in fact, induced.

Another procedure is the mixing of HIPS with poly(dimethylphenylene oxide) (PPO).[8,9] PPO is known to be very compatible with the PS matrix. The matrix strength of HIPS is increased by blending with PPO. This also leads to a state of very high hydrostatic pressure during tensile deformation, resulting in cold drawing. These relationships are schematized in Figure 7.

Then, ABS, of which the matrix consists of SAN, enhances the matrix strength of HIPS by the incorporation of a polar group, as in PPO. In the present study, the deformation mechanism of ABS was, however, limited to microcrazing

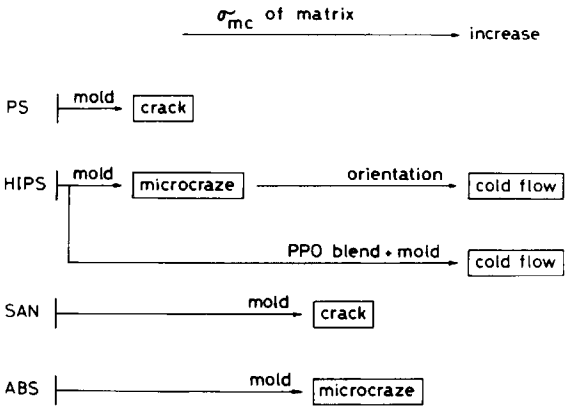

Fig. 7. Qualitative relationship between tensile deformation mechanism and critical microcrazing stress (σ_{mc}) among PS, SAN, HIPS, and ABS.

(whitening), and no shear band formation (cold drawing) was observed. This indicates that only the introduction of a polar group (as nitrile group) could not strengthen the matrix as much as preorientation or blending with PPO.

References

1. M. Yokouchi and Y. Kobayashi, *J. Appl. Polym. Sci.*, **24**, 29 (1979).
2. C. B. Bucknall and R. R. Smith, *Polymer*, **6**, 437 (1965).
3. H. Kawai, T. Hashimoto, M. Miyoshi, H. Uno, and M. Fujimura, *J. Macromol. Sci.*, **B17**, 427 (1980).
4. M. Yokouchi, H. Uchiyama, and Y. Kobayashi, *J. Appl. Polym. Sci.*, **25**, 1007 (1980).
5. K. Matsushige, S. V. Racliffe, and E. Baer, *J. Polym. Sci., Polym. Phys. Ed.*, **14**, 703 (1976).
6. K. Matsushige, S. V. Racliffe, and E. Baer, *J. Appl. Polym. Sci.*, **20**, 1853 (1976).
7. M. Yokouchi, A. Yokota, and Y. Kobayashi, *J. Appl. Polym. Sci.*, **27**, 3007 (1982).
8. C. B. Bucknall, I. C. Drinkwater, and W. E. Keast, *Polymer*, **13**, 115 (1972).
9. C. B. Bucknall, D. Clayton, and W. E. Keast, *J. Mater. Sci.*, **7**, 1443 (1972).

Received October 12, 1982
Accepted February 1, 1983